microorganisms

MDPI

Article

Isolation and Characterization of Two Ngari Virus Strains from Engorged Ixodid Ticks Collected from Cattle in Guinea

Roman B. Bayandin [1,*], Elena V. Protopopova [1], Anastasia V. Gladysheva [1], Victor A. Svyatchenko [1], Marat T. Makenov [2], Lyudmila S. Karan [2], Sanaba Boumbaly [3], Alexander P. Agafonov [1] and Vladimir A. Ternovoi [1]

[1] State Research Center of Virology and Biotechnology Vector, 630559 Koltsovo, Russia
[2] Central Research Institute of Epidemiology, Novogireevskaya St. 3A, 111123 Moscow, Russia
[3] Virology Research Center/Laboratory of Viral Hemorrhagic Fevers, Conakry P.O. Box 5680, Guinea
* Correspondence: bayandin_rb@vector.nsc.ru

Abstract

Ngari virus (NRIV) is a mosquito-borne reassortant orthobunyavirus associated with severe human disease in Africa. We isolated two NRIV strains, Tintin and Sabadou, from pools of engorged ixodid ticks collected from cattle in Guinea and characterized their genomes, replication in six cell lines, and pathogenicity in BALB/c mice. Tick vector competence was not assessed, and isolation from engorged ticks does not establish their role in NRIV transmission. Genome sequencing revealed close relationships with Mauritanian isolates and high sequence identity between the Guinean strains. Both strains replicated efficiently in mammalian cells and C6/36 mosquito cells, whereas replication in TH-1 turtle cells was limited. Cytopathic effects were observed in mammalian cells but not in C6/36 or TH-1 cells. Intracerebral inoculation resulted in 100% mortality in suckling mice for both strains at each tested dose (2.3 and 4.3 $\log_{10}$ $TCID_{50}$/mouse, where $TCID_{50}$ is the 50% tissue culture infectious dose). In adult mice inoculated intracerebrally at 4.3 $\log_{10}$ $TCID_{50}$/mouse, mortality was 80% for Tintin and 100% for Sabadou. Subcutaneous inoculation caused 20% and 40% mortality in adult mice, respectively. Exploratory survival analyses suggested a possible between-strain difference in adult mice inoculated intracerebrally. Viral RNA and infectious virus were detected in brain samples from the examined animals, including those inoculated subcutaneously, but were not detected in the other organs examined. These findings characterize the pathogenicity of the two isolates in BALB/c mice and are consistent with CNS involvement following peripheral inoculation, although tissue sampling from two animals per sampled group does not establish the frequency, kinetics, or route of neuroinvasion.

Keywords: Nagri virus; *Orthobunyavirus*; reassortment; phylogenetic analysis; Guinea; ixodid ticks; viral isolation; neurovirulence; neuroinvasiveness

Check for updates

Academic Editor: Simone Peletto

Received: 5 November 2026
Revised: 19 November 2026
Accepted: 21 November 2026
Published: 26 November 2026

Copyright: © 2026 by the authors. Licensee MDPI, Basel, Switzerland. This article is an open access article distributed under the terms and conditions of the Creative Commons Attribution (CC BY) license.

1. Introduction

Ngari virus (NRIV) belongs to the species *Orthobunyavirus bunyamweraense*, genus *Orthobunyavirus* (family *Peribunyaviridae*) [1]. It is a mosquito-borne virus with a segmented genome of negative-sense single-stranded RNA. NRIV is a natural reassortant of two closely related viruses: Bunyamwera virus (BUNV, *Orthobunyavirus bunyamweraense*) and Batai virus (BATV, *Orthobunyavirus bataiense*). The NRIV genome contains the L segment and S segment of BUNV, and the M segment of BATV. All three viruses (BUNV, NRIV, and BATV)

have been reported to infect humans and other mammals. In domestic animals, especially ruminants, infection can lead to severe symptoms, such as abortions, premature births, teratogenic effects, and hemorrhagic infection [2–5]. However, it was shown that reassortment in viruses of the order *Bunyavirales* can increase virulence [6,7]. Infection with NRIV results in more severe disease compared to BUNV and BATV and causes large outbreaks of disease in livestock [8,9]. NRIV is highly pathogenic to humans and was recognized as the cause of fatal hemorrhagic fever cases during an outbreak in Kenya and Somalia in 1997–1998 [6,10,11]. Therefore, in addition to its important veterinary significance, NRIV is of particular public health importance. NRIV has been isolated from mosquitoes belonging to several genera, including *Aedes*, *Anopheles*, and *Culex* [12–14]. Viral RNA or infectious virus has also been detected in engorged ticks, including *Amblyomma variegatum*, *Amblyomma gemma*, *Rhipicephalus geigyi*, *Rhipicephalus pulchellus*, and *Rhipicephalus* (*Boophilus*) spp.; however, vector competence of these ticks for NRIV has not been demonstrated [15,16]. Despite these reports of NRIV detection in different arthropods, its confirmed geographic distribution remains limited to Africa: Senegal, Guinea, Mauritania, Burkina Faso, Central African Republic, Sudan, Somalia, Kenya, Uganda, Democratic Republic of the Congo, Madagascar, and South Africa [6,8,13,15,17,18]. NRIV, like other *orthobunyaviruses*, has been isolated in monkey kidney cells (Vero), as well as on mosquito cells C6/36 (*Aedes albopictus*), sheep cells Llu-L, and on human cell line HEK293-T [18]. This provided opportunities to study the virus in laboratory conditions. In this study, we isolated two viable NRIV strains from previously identified PCR-positive tick pools and characterized their genome sequences, replication in mammalian, mosquito, and reptilian cell lines, and pathogenicity in mice. Intracerebral inoculation was used to assess neurovirulence, whereas subcutaneous inoculation was used to assess disease outcomes and evidence of CNS involvement following peripheral inoculation; suckling and adult mice were compared to assess age-dependent susceptibility, and tissues were examined to determine whether the virus is detectable outside the brain. Mice are widely used for this purpose and, as NRIV causes severe disease in humans [6,10,11], allow a first assessment of the pathogenic potential of the Guinean isolates, although mouse data cannot be directly extrapolated to humans. The mouse experiments were intended to describe disease outcomes following intracerebral and subcutaneous inoculation and to explore possible differences between the two isolates.

2. Materials and Methods

2.1. Cell Lines and Viruses

The ticks were collected from cattle in six regions of Guinea. The two NRIV isolates characterized in this study originated from pools of engorged ixodid ticks collected from cattle. Whole ticks were homogenized; tick tissues were not dissected. Tick collection, species identification, pooling criteria, and homogenization procedures were described previously [15]. NRIV was isolated on Vero cell culture. Vero cells (African green monkey kidney cells) (150–200 thousand cells in 1 mL) were cultured in a 25 cm^2 cell culture flask (Biologix, Jinan, China) with DMEM/F12 (1:1) medium (Thermo Fisher Scientific, Waltham, MA, USA) supplemented with 5% fetal bovine serum (Thermo Fisher Scientific, Waltham, MA, USA) and 200 µg/mL of penicillin and streptomycin (1:1) (Thermo Fisher Scientific, Waltham, MA, USA). The tick homogenates were centrifuged at 5000× *g* to remove debris. Vero cells were infected with 1 mL of a mixture of 100 µL of PCR-positive NRIV homogenate and 900 µL of DMEM/F12 medium (1:1) (prefiltered through a 0.45 µm filter) and were incubated for 1 h at 37 °C. They were then washed with phosphate-buffered saline and covered with DMEM/F12 containing 2% fetal bovine serum. Viral RNA signal was monitored by RT-qPCR. Aliquots for RT-qPCR were collected on days 8, 10, and 12. Ct values stabilized on days 10–12. On day 12, an aliquot of the culture supernatant was collected for

subsequent passage. The sequences deposited in GenBank were obtained from the second-passage virus stocks, which were also used in the cell-culture and mouse experiments. Each strain was grown individually to avoid cross-contamination, and supernatants were harvested when approximately 90% of the cells exhibited CPE. The culture supernatants were aliquoted and stored at −80 °C until use. The stock concentrations were determined by a 50% tissue culture infectious dose ($TCID_{50}$) assay. Vero cells were seeded in 96-well plates and incubated in a humidified CO_2 incubator at 37 °C overnight before use. The cells were used when they attained 80–90% confluence. Ten-fold dilutions of the virus-containing samples were prepared in maintenance medium. Medium was carefully aspirated from the wells, and 50 µL of the appropriate viral dilution was added to each of the triplicate wells of 96-well plates with gentle rocking to evenly distribute the virus. Plates were incubated at 37 °C for 1 h, after which the media were carefully aspirated, and 150 µL of DMEM/F12 with 2% fetal bovine serum was gently added to each well. Plates were incubated for 5 days in a humidified CO_2 incubator. The development of CPE was monitored by visualization under an inverted microscope. The infectious viral titers for NRIV strains were determined using a $TCID_{50}$ assay, as estimated by microscopic scoring of the CPE and by measuring cell viability in a formazan-based MTT assay. Further passages were carried out on Vero E6 (African green monkey kidney cells; ATCC CRL-1586), SPEV (swine embryonic kidney cells; Cellosaurus accession No. CVCL_4625), HEK293A (human embryonic kidney cells; Cellosaurus accession No. CVCL_6910), TH-1 (Eastern box turtle heart cells; ATCC CCL-50), and C6/36 (Aedes albopictus cells; ATCC CRL-1660). All cell lines used in this study, including Vero (African green monkey kidney cells; ATCC CCL-81), were obtained from the cell culture collection of the State Research Center of Virology and Biotechnology VECTOR (Koltsovo, Novosibirsk Oblast, Russia). The infectious viral titers for NRIV strains passaged on the cell cultures indicated above were determined in Vero cells using a $TCID_{50}$ assay, with a detection limit of 1.3 $\log_{10}TCID_{50}$/mL. Passage numbers for the cell culture samples are provided in Section 3.3. All work with infectious virus, including cell culture, was performed under biosafety level 3 (BSL-3) conditions.

2.2. Pathogenicity in Mice

Pathogenicity of the NRIV strains Tintin and Sabadou was evaluated in suckling BALB/c mice (2–3 days old) and six-week-old BALB/c (males, 21.4 ± 0.6 g; females, 18.2 ± 0.4 g) mice obtained from the animal facility of the SRC VB "Vector". The mice had not been used in any previous experiments and were pathogen-free. They were housed in plastic cages with dried birch wood shavings as bedding under a 12:12 h light/dark cycle and had free access to water and compound feed (ProKorm, BioPro, Novosibirsk, Russia). The animal room was maintained at approximately 22 °C and 35% relative humidity, and the acclimatization period was 7 days. All animal work was performed in an animal biosafety level 3 (ABSL-3) facility. Suckling mice were housed with the dam, ten pups per cage; adult mice were housed five per cage by sex, and each group of ten consisted of one cage of five males and one cage of five females. No environmental enrichment other than bedding was provided. In total, 110 mice were used: 50 suckling mice (from five litters) and 60 adult mice (equal numbers of males and females, housed separately by sex). The sex of suckling mice was not determined. Animals showing weight loss, poor coat condition, lethargy, loss of appetite or social withdrawal during acclimatization were not enrolled, together with their subgroup or litter. After acclimatization, adult mice homogeneous in age and body weight were randomly allocated to subgroups of five animals using a random number generator in Excel, and male and female subgroups were then randomly combined into groups of ten (five males and five females). Suckling mice from different litters were randomized and distributed across the groups in a mixed manner to control for

the litter effect. The same random number generator was used for suckling mice. The order of inoculation within groups and the order in which cages were handled were random; cage position in the room was not randomized. The experimental unit was the individual animal, and all enrolled animals were included in the survival analyses. No criteria for excluding animals after the start of the experiment or data points from the analysis were set, and no animals were excluded. Inoculation and clinical assessment were performed by different investigators. The observer performing the clinical assessment was unaware of the group allocation. The investigator who analyzed the data was also unaware of the group allocation. Suckling mice were inoculated intracerebrally with 4.3 $\log_{10}$TCID$_{50}$/mouse ($n = 10$ per strain) or 2.3 $\log_{10}$TCID$_{50}$/mouse ($n = 10$ per strain) in a volume of 20 µL per mouse. Adult BALB/c mice were inoculated intracerebrally with 4.3 $\log_{10}$TCID$_{50}$/mouse in a volume of 20 µL ($n = 10$ per strain) or subcutaneously with 5.3 $\log_{10}$TCID$_{50}$/mouse in a volume of 200 µL ($n = 10$ per strain). Second-passage virus stocks were diluted in PBS. Prior to inoculation, adult mice were anesthetized with Zoletil (20 mg/kg) and xylazine (5 mg/kg). Before inoculation, each suckling mouse was placed in a 5-mL tube, which was immersed in an ice–water bath maintained at 2–4 °C, with the water level approximately corresponding to the animal's neck. The animal remained dry, without direct contact with water or ice. Cooling lasted 5–8 min. Anesthetic depth was assessed by the absence of a withdrawal response to a firm toe pinch. Skin pallor and absence of the righting reflex were also monitored. Immediately before inoculation, the animal was placed on a plastic Petri dish positioned on ice. Following inoculation, the animal was immediately transferred to a warming pad maintained at 33–37 °C and monitored until normal pink skin coloration and spontaneous activity had returned. Separate age-matched control groups ($n = 10$ per group) received PBS via the corresponding inoculation routes: 20 µL intracerebrally for suckling and adult mice and 200 µL subcutaneously for adult mice. Survival (Kaplan–Meier curves, log-rank test) was the primary outcome. No a priori sample size calculation was performed; a group size of $n = 10$ was chosen in line with established practice in virulence studies, in accordance with the Reduction principle of the 3Rs, and allowing for possible procedure-related losses in the intracerebrally inoculated groups. All animals were observed twice daily for 14 days (336 h) for clinical signs, including piloerection, hunched posture, uncoordinated gait, tremors, hind-limb dragging, and death. Immediately after inoculation, animals were inspected several times a day. Adult mice showing these signs were euthanized by cervical dislocation; suckling mice showing these signs or burrowing into the bedding were euthanized by cooling followed by decapitation (humane endpoints). Before decapitation, suckling mice underwent the same cooling procedure described above, and absence of a withdrawal response to a firm toe pinch was confirmed. At the end of the observation period, surviving animals from the neonatal cohort, including the PBS controls, were approximately 16–17 days old. These animals received the same pharmacological anesthesia as adult mice, with the administered amounts calculated according to individual body weight, followed by euthanasia by cervical dislocation. The neonatal cooling procedure was not used for these older animals. Surviving adult mice were euthanized using the procedure described above for adults. Animals euthanized at humane endpoints were recorded as deaths in the survival analysis. Individual animal survival data, including the PBS control groups, are provided in Supplementary Table S2 (adult mice) and S3 (suckling mice). Each record includes the animal identifier, strain or PBS treatment, dose, inoculation route, observation time in hours, and event indicator. Death or euthanasia at a humane endpoint was coded as 1; survival to the end of follow-up was coded as 0, with right-censoring at 336 h. Animals found dead or euthanized at humane endpoints were necropsied immediately after inspection. Tissue samples were collected from two deceased animals per group for the tissue analyses reported in Section 3.4: suckling mice inoculated intracerebrally with 4.3 $\log_{10}$TCID$_{50}$/mouse

and adult mice inoculated intracerebrally with 4.3 $\log_{10}$TCID$_{50}$/mouse or subcutaneously with 5.3 $\log_{10}$TCID$_{50}$/mouse, for each strain. For each organ, equal-mass tissue samples from the two animals were homogenized separately. RT-qPCR was performed on the individual tissue homogenates before pooling. Infectivity of the individual homogenates was assessed by CPE in Vero cells before pooling. Equal-volume aliquots (50 µL) of the corresponding homogenates from each animal were pooled and mixed thoroughly to obtain one pooled sample per organ and group. Each pooled sample was titrated in Vero cells in three replicate assays using 10-fold serial dilutions, and the 50% tissue culture infectious doses were calculated using the Spearman–Karber method [19]. Samples that produced no CPE in any inoculated well, including at the lowest dilution tested, were reported as below the infectivity-assay detection limit of 1.3 $\log_{10}$TCID$_{50}$/mL. All animal procedures were conducted in accordance with the "Rules for carrying out work using experimental animals" (https://docs.cntd.ru/document/456016716, accessed on 21 April 2021), the Guide for the Care and Use of Laboratory Animals [20], and protocol No. 1-04.2021 approved by the Bioethics Commission of the SRC VB "Vector" on 30 April 2021. The experimental design was defined in this approved protocol; the study was not registered in a public registry. This study is reported in accordance with the ARRIVE 2.0 guidelines [21].

2.3. RNA Isolation and Reverse Transcription

The internal organs of mice were homogenized using a TissueLyser LT homogenizer (QIAGEN, Hilden, Germany). Next, RNA was isolated from 100 µL of the tissue homogenate or cell suspension using TRIzol reagent (Thermo Fisher Scientific, Waltham, MA, USA) according to the manufacturer's instructions. cDNA was synthesized using the commercial REVERTA-L RT kit (AmpliSens, Central Research Institute of Epidemiology, Moscow, Russia) according to the manufacturer's instructions.

2.4. PCR and Sequencing

Viral RNA was detected by quantitative PCR following reverse transcription (RT-qPCR), using the primers NgvS-F2 and NgvS-R2 and the probe NgvS-proba2, under the conditions described previously [15]. The detection limit of the infectivity assay was 1.3 $\log_{10}$TCID$_{50}$/mL. A formal analytical detection limit was not established for RT-qPCR. Further, the genome sequence for each strain was obtained using the Sanger method. Primers for the complete genome amplification are presented in Table S1. Complete genome PCR was carried out using the PCRmix-HS mixture (Evrogen, Moscow, Russia) under the following conditions: (I) 95 °C for 5 min; (II) 40 cycles of 95 °C for 10 s, 55 °C for 30 s, and 72 °C for 30 s; and (III) 72 °C for 5 min. Subsequent sequencing was performed with a panel of primers (Table S1) using the BigDye Terminator v3.1 Cycle Sequencing Kit (Thermo Fisher Scientific, Waltham, MA, USA) on an Applied Biosystems 3500xL Genetic Analyzer (Applied Biosystems, Thermo Fisher Scientific, Waltham, MA, USA). The deposited sequences were obtained from the same second-passage virus stocks used in the cell-culture and mouse experiments. Post-passage sequencing detected a limited number of nucleotide substitutions relative to the inoculum stocks. These sequence data are reserved for a separate report. The terminal sequences of the three genomic segments were not independently validated; therefore, the accuracy and completeness of the segment termini remain unconfirmed. The genome sequences have been deposited in GenBank under the following accession numbers: for the Tintin strain, MT929317 (L segment), MT929318 (M segment), and MT929319 (S segment); for the Sabadou strain, MT929320 (L segment), MT929321 (M segment), and MT929322 (S segment).

2.5. Phylogenetic Analysis

All complete genome sequences of Bunyamwera virus (BUNV), Batai virus (BATV), and Ngari virus (NRIV) available in GenBank at the time of retrieval in November 2023 were included in the phylogenetic analysis. Five strains labelled as Calovo virus were also included and treated as BATV, consistent with their classification in the previous study [22]. The alignment of nucleotide sequences was performed using MEGA X [23]. Nucleotide substitution models were selected automatically using the model-selection procedure implemented in IQ-TREE v1.6.12. Maximum-likelihood phylogenies were inferred using the selected HKY+F+G4, GTR+F+I+G4, and TN+F+I+G4 models for the S-, M-, and L-segment alignments, respectively. Support for the tree was assessed with 1000 ultrafast bootstrap replicates [24]. The consensus trees were reconstructed with IQ-TREE v1.6.12 [25] and visualized in iTOL v6.6 (https://itol.embl.de, accessed on 6 March 2024).

2.6. Statistical Analysis

Survival curves were estimated using the Kaplan–Meier method over the complete 336-h observation period. Survival distributions between the Tintin and Sabadou strains were compared using the log-rank (Mantel–Cox) test within groups matched for animal age, inoculation route, and virus dose. All analyses were performed in R (version 4.4.2) with the following packages: 'survival' [26] for constructing Kaplan–Meier estimators and log-rank tests, and 'survminer' [27] and 'ggplot2' [28] for data visualization. Pointwise 95% confidence intervals for the Kaplan–Meier survival curves were calculated using Greenwood's variance formula with a log–log transformation (conf.type = "log-log"). The 95% confidence limits for median survival times were obtained by inverting these confidence limits at a survival probability of 0.5 (Brookmeyer–Crowley approach). Surviving animals were right-censored at 336 h. Censoring was administrative only (survivors at the end of the fixed observation period), and no animals were lost to follow-up, so censoring was independent of the outcome. No Cox proportional hazards model was fitted, and proportional hazards were not formally assessed. When the estimated survival curve had a plateau at 0.5, the midpoint of the plateau was reported as the median, consistent with the 'survival' R package. Viral titers of the Tintin and Sabadou strains within each cell line were compared using Student's t-test. Titers were analyzed on the $\log_{10}$ scale; because only three independent experiments were available per cell line, normality and equality of variances could not be meaningfully tested. For the exploratory between-strain comparisons, $p < 0.05$ was used as a nominal threshold. Reported p-values were not adjusted for multiple comparisons. Given the small group sizes and multiple comparisons, p-values were interpreted cautiously; non-significant results were not considered evidence of equivalence between the strains.

3. Results

3.1. Two NRIV Strains Were Successfully Isolated from Tick Pools

In our previous study, a total of 710 pools (2067 ticks) of various tick species were collected from six regions of Guinea, and PCR testing detected NRIV RNA in 12 of these pools [15]. In the present study, Vero cell cultures were inoculated with homogenates from these 12 PCR-positive tick pools, which comprised *Am. variegatum*, *Rh. geigyi*, and *Rh.* (*Boophilus*) spp. Two strains of NRIV were successfully isolated from two distinct pools of engorged ixodid ticks collected from cattle (*Rh.* (*Boophilus*) spp. and *Rh. geigyi*) from Tintin (10°13′00″ N, 9°12′00″ W) and Sabadou (10°07′48″ N, 8°45′45″ W) villages in Kankan region. During primary inoculation, neither strain exhibited a cytopathic effect (CPE), and viral replication was detectable exclusively by RT-qPCR in the culture supernatant. The initial tick homogenates yielded Ct values of 29.51 for Tintin and 32.01 for Sabadou.

Aliquots were collected for RT-qPCR analysis on days 8, 10, and 12 post-inoculation. During virus propagation, Ct values decreased and stabilized by days 10–12. On day 12, Ct values reached 13.04 for Tintin and 15.93 for Sabadou, indicating a marked increase in the viral RNA signal relative to the initial tick homogenates. The culture supernatants were then harvested for subsequent passage. Sequencing was performed on the resulting second-passage virus stocks used in the cell-culture and mouse experiments. Upon the second passage in Vero cells, initial signs of CPE were recorded between 48 and 60 h post-infection, progressing to complete cell lysis by day 5. The infectious titers of the resulting viral stocks were determined to be about 7.0 $\log_{10}$TCID$_{50}$/mL.

3.2. Guinean NRIV Strains Are Closely Related to Mauritanian Isolates

During whole-genome sequencing of the obtained strains, segments of the following lengths were assembled: 6876 nt for the L segment, 4439 nt for the M segment, and 954 nt for the S segment. For phylogenetic analysis, only the open reading frames of each segment (6717, 4305, and 702 nt) were used (Figures 1–3). The segment phylogenies were consistent with the established reassortant ancestry of NRIV, with BUNV-related S and L segments and a BATV-related M segment. The Guinean strains showed the highest sequence identity to each other, with nucleotide p-distances of only 0.19% for the L segment and 0.16% for the M segment, while their S segments were identical. This high level of sequence similarity indicates a close genetic relationship between the two Guinean isolates but does not establish a shared epidemiological source or the timing, direction, or number of introduction events. On the phylogenetic trees of the L, M, and S segments, the Guinean strains (Tintin and Sabadou) clustered with Mauritanian strains and the 2020 Kenyan isolates. Within this clade, they exhibited the highest sequence similarity to the 2015 Mauritanian strains (15Guidimaka/ME and 428Trarza/ME), followed by the 2010 Adrar strain, while showing lower sequence identity to the 2020 Kenyan strains in the L and M segments. Specifically, sequence identity to the 2015 isolates ranged from 98.93–98.97% for the L segment, 99.19–99.30% for M, and 99.86–100% for S. For the Adrar strain, these values were 98.54% (L), 98.12–98.16% (M), and 99.15% (S), whereas sequence identity to the Kenyan strains was 98.04–98.09% (L), 97.72–97.84% (M), and 99.72% (S). For the 702-nt nucleoprotein coding region of the S segment, both Guinean strains differed from each of the four 2020 Kenyan isolates by two nucleotides (99.72% identity), compared with six nucleotide differences from Adrar (99.15% identity). Moreover, Omoga et al. reported that the four Kenyan NRIV isolates shared a most recent common ancestor (MRCA) with the Adrar strain isolated in Mauritania in 2010 [18]. In contrast, the Tintin and Sabadou strains were most closely related to 15Guidimaka/ME and 428Trarza/ME. Taken together, these findings demonstrate a close phylogenetic relationship among the Guinean, Mauritanian, and Kenyan NRIV strains. However, the geographic origin of the Guinean strains and the timing, direction, and number of introduction events cannot be resolved from the available data.

3.3. Tintin and Sabadou Replicate Efficiently in Mammalian Cell Lines

When Vero, Vero E6 (African green monkey kidney), HEK293A (human kidney), SPEV (pig embryo kidney), C6/36 (*Aedes albopictus*), and TH-1 (Eastern box turtle heart) cell lines were infected with second-passage NRIV at a multiplicity of infection (MOI) of 0.1 TCID$_{50}$/cell, CPE appeared after 48 h in Vero, Vero E6, and HEK293A cells, and after 60 h in SPEV cells. In contrast, no CPE was observed in C6/36 or TH-1 cells during their respective observation periods of 7 and 10 days (Table 1). The later harvest times for C6/36 and TH-1 cells were selected following preliminary observations. At the sampling time used for Vero cells, RT-qPCR showed low viral RNA signals in these cultures, and no cytopathic effects were observed. These observations prompted later collection of the C6/36

and TH-1 culture supernatants. Accordingly, the resulting titers represent measurements at the selected endpoints rather than a standardized comparison of replication kinetics across cell lines. To compare infectious virus production across these cell lines, culture supernatants were collected on day 5 of incubation (and on days 7 and 10 for C6/36 and TH-1 cells, respectively), and infectious titers were determined using Vero cells. The highest NRIV titers (~7.0–8.0 $\log_{10}$TCID$_{50}$/mL) were detected in Vero, Vero E6, HEK293A, and SPEV cells; the titer for C6/36 cells was approximately 6.0 $\log_{10}$TCID$_{50}$/mL, whereas for TH-1 cells it was less than 3.0 $\log_{10}$TCID$_{50}$/mL (Table 1).

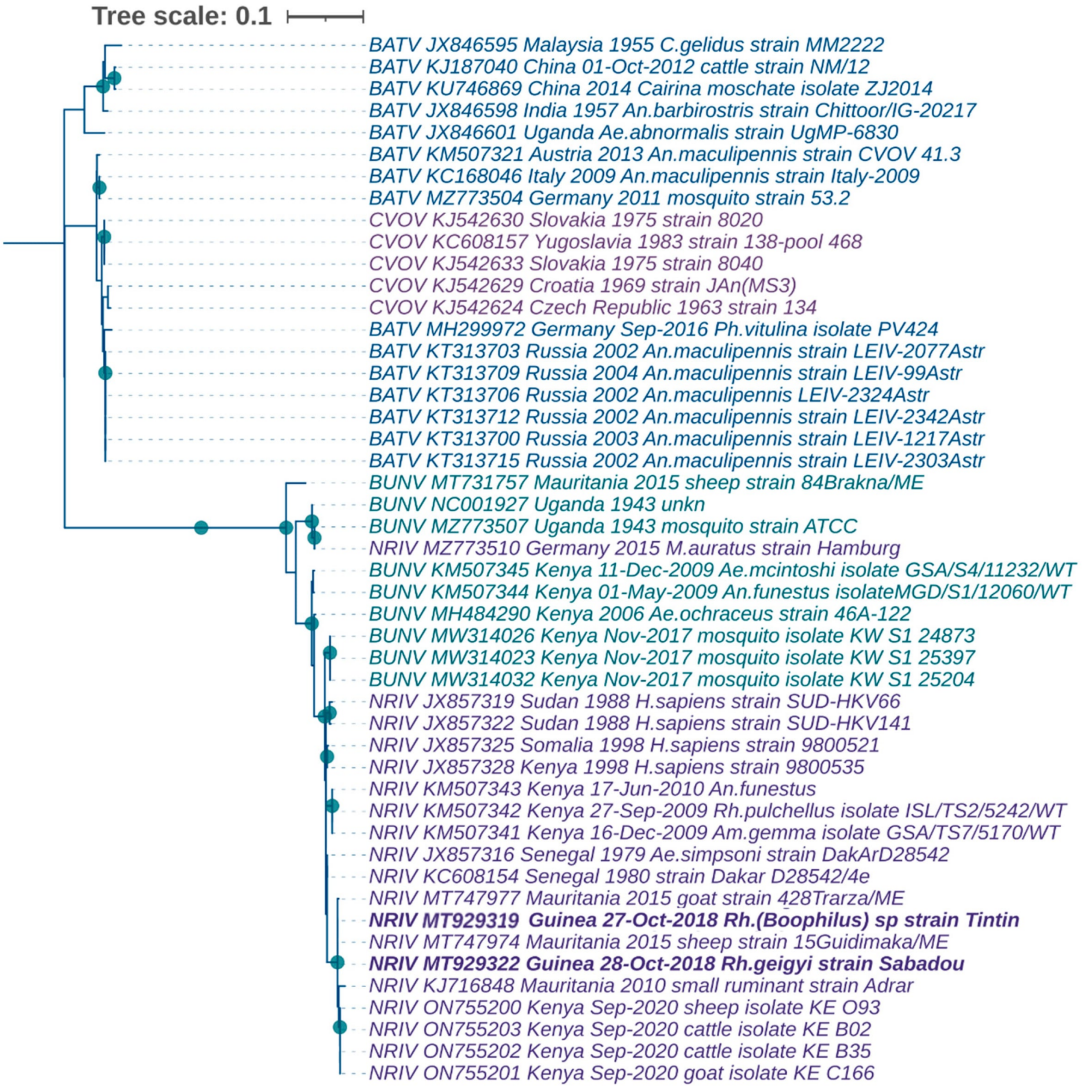

Figure 1. Maximum-likelihood (ML) phylogeny of the S-segment based on 49 sequences and 702 nucleotide sites. The ML tree was inferred with the HKY+F+G4 substitution model and a gamma-distributed rate heterogeneity with four categories (shape parameter $\alpha = 0.2103$). Branch support was assessed with 1000 bootstrap replicates; only values > 0.9 are shown as filled circles on branches. The tree was rooted using the La Crosse virus (GenBank accession NC_077808) as an outgroup; the outgroup sequence was removed from the figure to avoid compressing the terminal branches and to improve readability. The scale bar represents the mean number of nucleotide substitutions per site.

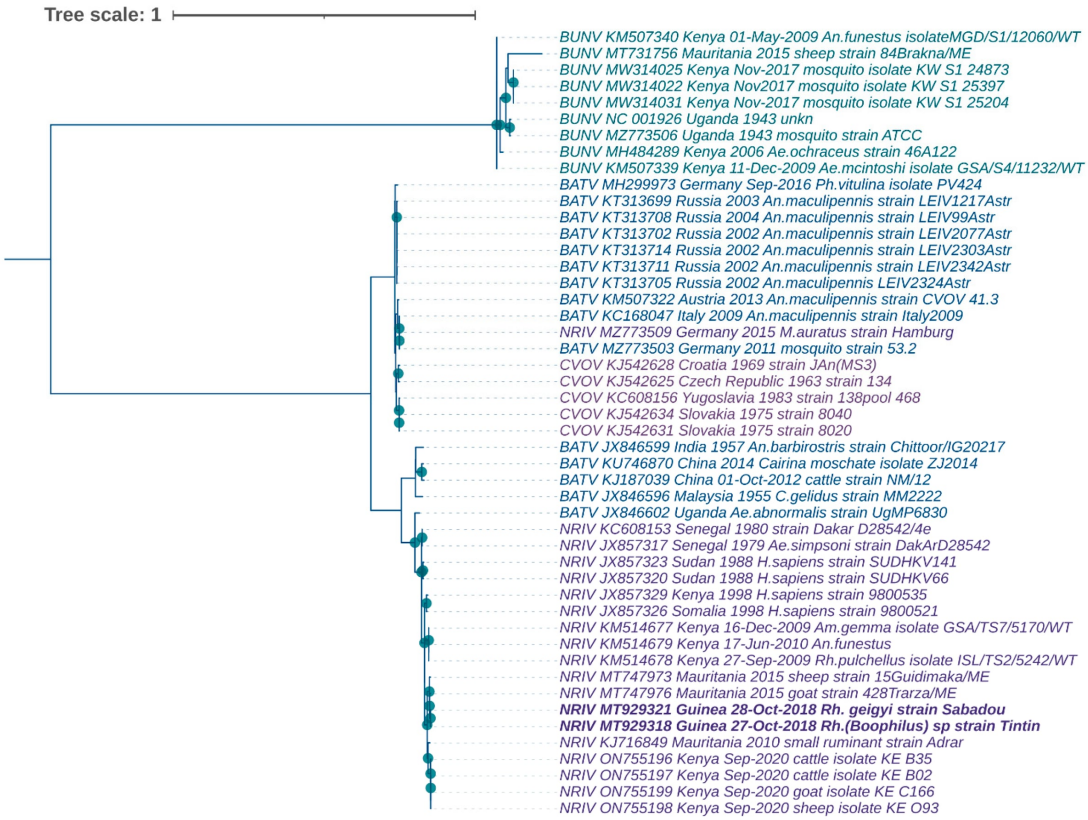

Figure 2. Maximum-likelihood (ML) phylogeny of the M-segment based on 49 sequences and 4305 nucleotide sites. The ML tree was inferred with the GTR+F+I+G4 substitution model and a gamma-distributed rate heterogeneity with four categories (shape parameter $\alpha = 0.8303$). Branch support was assessed with 1000 bootstrap replicates; only values >0.9 are shown as filled circles on branches. The tree was rooted using the La Crosse virus (GenBank accession NC_077809) as an outgroup; the outgroup sequence was removed from the figure to avoid compressing the terminal branches and to improve readability. The scale bar represents the mean number of nucleotide substitutions per site.

Table 1. In vitro replication activity of the NRIV strains.

Cell Line/ Organism/ Passage No.	CPE	Harvest Day	Viral Titers, $\log_{10}$TCID$_{50}$/mL	
			Tintin	Sabadou
Vero/monkey/3	Present (at 48 h)	5	7.2 ± 0.3	7.0 ± 0.2
Vero E6/monkey/1	Present (at 48 h)	5	7.1 ± 0.4	6.7 ± 0.3
HEK293A/human/1	Present (at 48 h)	5	7.5 ± 0.4	8.1 ± 0.3
SPEV/swine/1	Present (at 60 h)	5	7.4 ± 0.3	7.6 ± 0.2
C6/36/mosquito/1	Absent	7	5.7 ± 0.3	6.0 ± 0.2
TH-1/turtle/1	Absent	10	2.4 ± 0.2	2.7 ± 0.3

Note: NRIV, Ngari virus; CPE, cytopathic effect; TCID$_{50}$, 50% tissue culture infectious dose. Viral titers are expressed as $\log_{10}$TCID$_{50}$/mL (detection limit, 1.3 $\log_{10}$TCID$_{50}$/mL). The passage number is given for each cell line in the first column. Data are presented as means ± standard deviation (SD) of three independent experiments. Pairwise comparisons between Tintin and Sabadou viral titers within each individual cell line were performed using Student's t-test. No statistically significant differences were found between the two strains across all tested cell lines ($p > 0.05$).

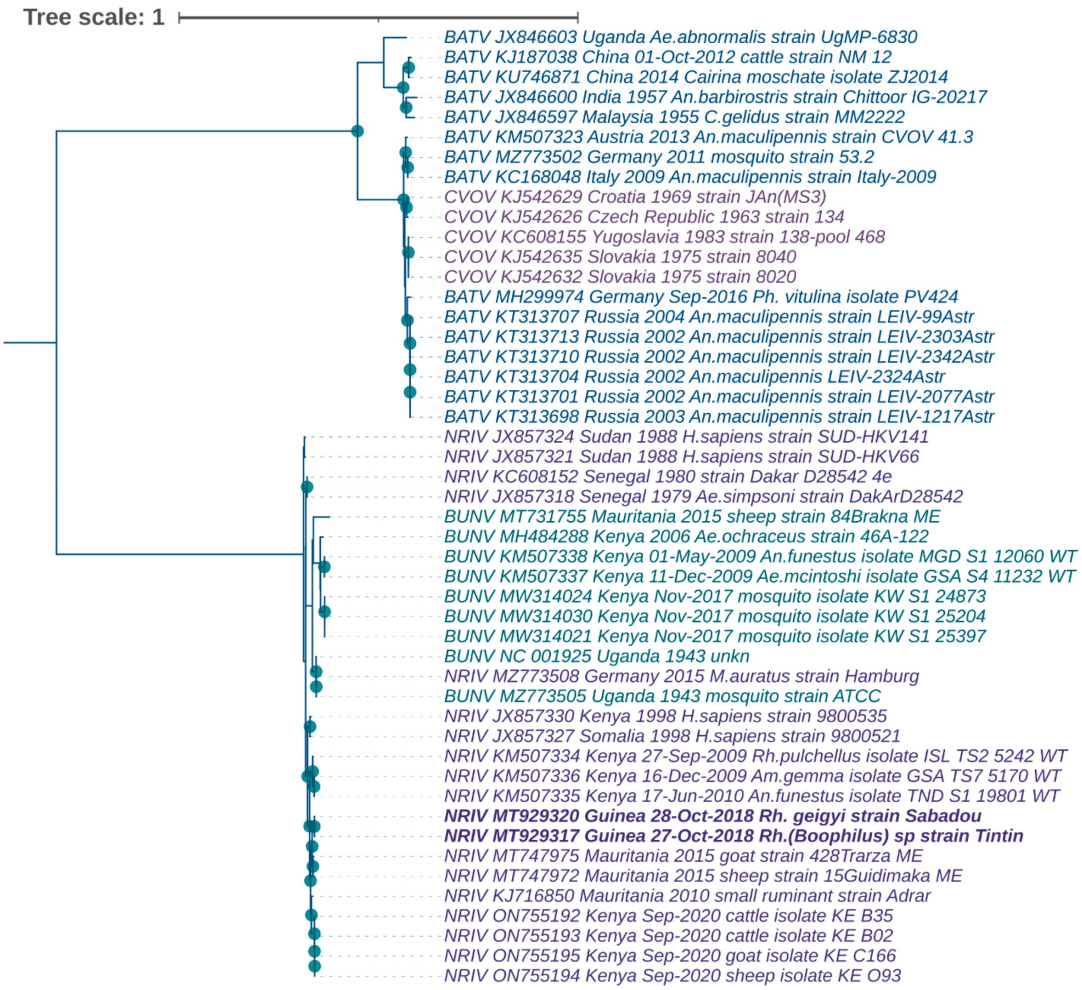

Figure 3. Maximum-likelihood (ML) phylogeny of the L-segment based on 49 sequences and 6717 nucleotide sites. The ML tree was inferred with the TN+F+I+G4 substitution model and a gamma-distributed rate heterogeneity with four categories (shape parameter $\alpha = 0.8514$). Branch support was assessed with 1000 bootstrap replicates; only values >0.9 are shown as filled circles on branches. The tree was rooted using the La Crosse virus (GenBank accession NC_077810) as an outgroup; the outgroup sequence was removed from the figure to avoid compressing the terminal branches and to improve readability. The scale bar represents the mean number of nucleotide substitutions per site.

3.4. Pathogenicity and Tissue Findings in BALB/c Mice

The pathogenicity of the isolated strains was studied in suckling and adult mice. Intracerebral infection of suckling mice with doses of 2.3 $\log_{10}TCID_{50}$/mouse or 4.3 $\log_{10}TCID_{50}$/mouse resulted in 100% mortality by 5–6 days (Figure 4A,B). Intracerebral infection of adult mice with the Tintin and Sabadou strains at a dose of 4.3 $\log_{10}TCID_{50}$/mouse resulted in 80% and 100% mortality, respectively, by day 9 (Figure 4C). Following subcutaneous inoculation with 5.3 $\log_{10}TCID_{50}$/mouse, clinical signs of infection, including piloerection, hunched posture, uncoordinated gait, tremors, and hind-limb dragging, were observed in 20% of mice infected with the Tintin strain and 40% of mice infected with the Sabadou strain; all affected animals died by day 9 post-infection (Figure 4D). All PBS-inoculated control animals survived the 336-h observation period without clinical signs of disease. In suckling mice, median survival times ranged from 90 to 114 h, depending on the strain and virus dose. In adult mice inoculated intracerebrally, median survival times were 168 h for the Sabadou strain and 210 h for the Tintin strain. Following subcutaneous in-

oculation, median survival was not reached for either strain because survival remained above 50% throughout the observation period (Table 2). Survival distributions of the Tintin and Sabadou strains were compared within groups matched for animal age, inoculation route, and virus dose. No statistically significant differences between the strains were detected in suckling mice inoculated intracerebrally with 4.3 $\log_{10}$TCID$_{50}$/mouse (log-rank $p = 0.171$) or 2.3 $\log_{10}$TCID$_{50}$/mouse ($p = 0.393$). Exploratory between-strain comparisons in adult mice yielded log-rank p-values of 0.024 following intracerebral inoculation with 4.3 $\log_{10}$TCID$_{50}$/mouse and 0.290 following subcutaneous inoculation with 5.3 $\log_{10}$TCID$_{50}$/mouse (Figure 4).

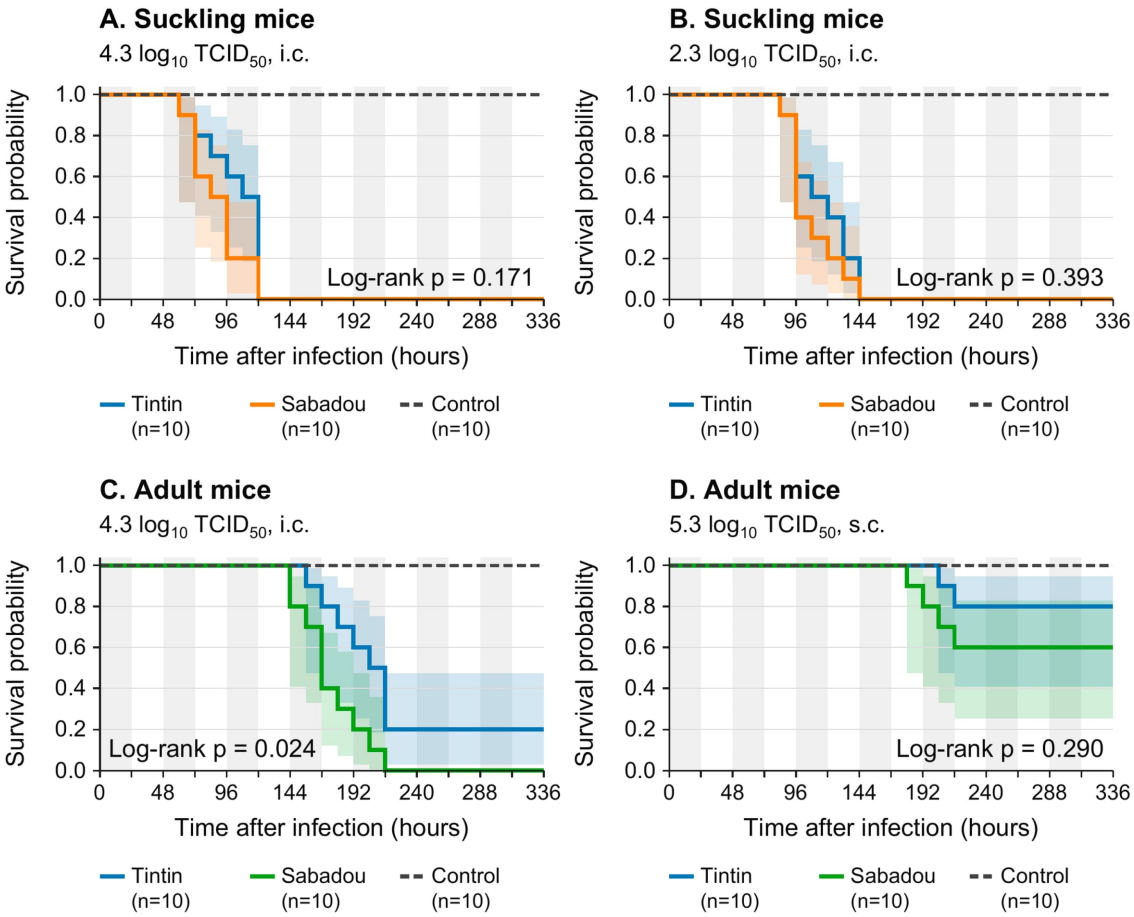

Figure 4. Kaplan–Meier survival curves for mice infected with NRIV strains Tintin and Sabadou. In each panel, survival probability is plotted against time (hours post-infection). Thick step lines represent Kaplan–Meier estimates, and shaded ribbons indicate pointwise 95% confidence intervals calculated using Greenwood's variance formula with a log–log transformation. Alternating light-grey and white background bands represent 24-h intervals. Survival distributions between the Tintin and Sabadou strains were compared using the log-rank (Mantel–Cox) test within groups matched for animal age, inoculation route, and virus dose, with p-values shown in the corresponding panels. All animals were alive at time zero. Age-matched PBS-inoculated control groups are shown in each panel; no deaths occurred in these groups during the 336-h observation period. Censored observations were included in the analysis. (**A**) Suckling mice, 4.3 $\log_{10}$TCID$_{50}$/mouse, intracerebral inoculation; (**B**) suckling mice, 2.3 $\log_{10}$TCID$_{50}$/mouse, intracerebral inoculation; (**C**) adult mice, 4.3 $\log_{10}$TCID$_{50}$/mouse, intracerebral inoculation; (**D**) adult mice, 5.3 $\log_{10}$TCID$_{50}$/mouse, subcutaneous inoculation.

Table 2. Kaplan–Meier estimates of median survival time with 95% confidence intervals.

Groups	Strain	Dose, $log_{10}TCID_{50}$/Mouse	Injection Route	Median, h	95% CI	Deaths/Total
Adult	Sabadou	4.3	Intracerebral	168	144–192	10/10
Adult	Sabadou	5.3	Subcutaneous	NR	180–NA	4/10
Adult	Tintin	4.3	Intracerebral	210	156–216	8/10
Adult	Tintin	5.3	Subcutaneous	NR	204–NA	2/10
Suckling	Sabadou	2.3	Intracerebral	96	84–120	10/10
Suckling	Sabadou	4.3	Intracerebral	90	60–96	10/10
Suckling	Tintin	2.3	Intracerebral	114	84–132	10/10
Suckling	Tintin	4.3	Intracerebral	114	60–NA	10/10

Note: Deaths/Total indicates the number of mice that died or were euthanized at a humane endpoint during the 336-h observation period relative to the total number of mice in each group. $TCID_{50}$, 50% tissue culture infectious dose; CI, confidence interval; NR, median survival time not reached because the estimated survival probability remained above 50% throughout the observation period; NA, the corresponding confidence limit could not be estimated by inversion of the log–log-transformed Greenwood confidence limits. A lower confidence limit may be estimable even when the median is not reached.

Internal organs (brain, liver, spleen, lungs, and kidneys) were harvested from animals in each group to analyze the presence of viral RNA and infectious NRIV (Table 3). All infectious virus titers in tissue homogenates were determined by titration on Vero cells. The highest viral titers were detected in suckling mice infected intracerebrally with 4.3 $log_{10}TCID_{50}$/mouse, reaching 8.0 ± 0.3 $log_{10}TCID_{50}$/mL for the Tintin strain and 9.0 ± 0.4 $log_{10}TCID_{50}$/mL for the Sabadou strain. In adult mice infected intracerebrally with the same dose (4.3 $log_{10}TCID_{50}$/mouse), the infectious titers in the brain were 7.0 ± 0.3 $log_{10}TCID_{50}$/mL for the Tintin strain and 7.1 ± 0.4 $log_{10}TCID_{50}$/mL for the Sabadou strain. In adult mice infected subcutaneously with 5.3 $log_{10}TCID_{50}$/mouse, the infectious NRIV titers in the brain were 3.9 ± 0.2 $log_{10}TCID_{50}$/mL (Tintin) and 4.0 ± 0.3 $log_{10}TCID_{50}$/mL (Sabadou). In the pooled tissue samples examined, regardless of the strain and infection route, viral RNA and infectious virus were detected exclusively in the brain, while all other organs remained negative. PCR analysis of viral RNA yielded identical positive and negative results across all analyzed tissues. Tissue samples were examined by both RT-qPCR and virus isolation in Vero cells, with concordant results: viral RNA and infectious virus were detected in brain samples, whereas samples from the other organs examined were negative by both methods. Infectious virus titers were subsequently determined in pooled tissue samples using Vero cells.

Table 3. Tissue distribution and infectious titers of NRIV in infected mice.

Tissue	Suckling Mice i.c., Dose (4.3 $log_{10}TCID_{50}$/Mouse), Vero		Adult Mice i.c., Dose (4.3 $log_{10}TCID_{50}$/Mouse), Vero		Adult Mice s.c., Dose (5.3 $log_{10}TCID_{50}$/Mouse), Vero	
	Tintin	Sabadou	Tintin	Sabadou	Tintin	Sabadou
Brain	8.0 ± 0.3	9.0 ± 0.4	7.0 ± 0.3	7.1 ± 0.4	3.9 ± 0.2	4.0 ± 0.3
Liver	–	–	–	–	–	–
Kidneys	–	–	–	–	–	–
Spleen	–	–	–	–	–	–

Table 3. *Cont.*

Tissue	Suckling Mice i.c., Dose (4.3 $\log_{10}$TCID$_{50}$/Mouse), Vero		Adult Mice i.c., Dose (4.3 $\log_{10}$TCID$_{50}$/Mouse), Vero		Adult Mice s.c., Dose (5.3 $\log_{10}$TCID$_{50}$/Mouse), Vero	
	Tintin	**Sabadou**	**Tintin**	**Sabadou**	**Tintin**	**Sabadou**
Lungs	–	–	–	–	–	–

Note: NRIV, Ngari virus; CPE, cytopathic effect; RT-qPCR, reverse transcription quantitative PCR; TCID$_{50}$, 50% tissue culture infectious dose. Viral titers are expressed as $\log_{10}$TCID$_{50}$/mL (infectivity-assay detection limit, 1.3 $\log_{10}$TCID$_{50}$/mL). The doses in the column headings are inoculation doses, expressed per mouse, rather than tissue titers. Data are presented as means ± standard deviation (SD) of three replicate titration assays of each pooled sample. For each organ, equal-mass tissue samples from two mice per group were homogenized separately, and 50 µL of each corresponding homogenate was pooled and mixed thoroughly. The SD describes variation between replicate assays of the pooled sample, rather than variation between individual animals. i.c., intracerebral inoculation; s.c., subcutaneous inoculation; "–", infectious virus was not detected by titration in Vero cells because no CPE was observed in any inoculated well, including at the lowest dilution tested; these results are reported as below the infectivity-assay detection limit of 1.3 $\log_{10}$TCID$_{50}$/mL. Infectious virus titers in tissue homogenates were determined in Vero cells using 10-fold serial dilutions, calculated by the Spearman–Karber method [19]. A formal analytical detection limit was not established for RT-qPCR. RT-qPCR analysis described in Section 2.4 yielded results concordant with virus titration: viral RNA was detected exclusively in brain tissue and was not detected in the other analyzed organs (liver, spleen, lungs, and kidneys).

4. Discussion

This study provides the first data on the isolation of two viable NRIV strains circulating in Guinea. The strains were isolated from two pools of engorged ixodid ticks (*Rhipicephalus geigyi* and *Rh. (Boophilus)* spp.) collected from cattle in two villages within the Kankan region. Our previous study reported the detection of NRIV RNA in engorged ticks collected from cattle in Guinea and confirmation of viral identity by sequencing short fragments of the S and M segments [15]. The present study extends those molecular findings by reporting the isolation of two viable NRIV strains from the previously identified PCR-positive tick pools and their genomic and biological characterization. Virus isolation was followed by genome sequencing and deposition of the sequences in GenBank (MT929317–MT929322), before the subsequent cell-culture and mouse studies reported here. Mosquito-borne viruses, including NRIV, Semliki Forest virus, West Nile virus, Bunyamwera virus, and Ndumu virus, have previously been detected in various tick species [16,29,30]. However, there is currently no evidence that ticks are competent vectors of NRIV, and isolation of the virus from engorged ticks does not establish their role in NRIV transmission. The recovered virus could have originated from the cattle blood meal; the present study did not determine whether the virus was present in tick tissues or in the ingested blood.

Because consensus Sanger sequencing was used, the presence of low-frequency variants in the original tick pools cannot be completely excluded. Across all three segments, the highest nucleotide sequence identity was observed with Mauritanian strains. These included the 15Guidimaka/ME and 428Trarza/ME strains isolated in 2015 and the Adrar strain isolated in 2010. Sequence identity to Adrar was higher than to the Kenyan isolates for the L and M segments, whereas the opposite was observed for the S-segment nucleoprotein coding region [8,9]. Detection of NRIV during outbreaks in Mauritania in 2010 and 2015 suggests recurrent virus circulation in the country. Phylogenetic analysis of four strains obtained during a 2020 livestock survey in Kenya showed that they formed a monophyletic group closely related to the Adrar strain isolated in Mauritania in 2010 [18]; however, these findings do not establish the direction of virus spread between Mauritania and Kenya. In Guinea, NRIV was also detected by our team in the Kindia region, located at a considerable

distance from the Kankan region [15]. Comparison of short fragments of the S- and M-segment genes (332 and 346 bp, respectively) showed that the Kindia sequences had the highest nucleotide identity with the Tintin and Sabadou strains, whereas their identity with other known NRIV strains was lower. The similarity of the available short S- and M-segment sequences indicates that genetically related NRIV sequences were detected in both the Kankan and Kindia regions [15]. However, these partial sequences do not establish a shared epidemiological source or a single introduction event. Likewise, the close relationship of the Guinean isolates to the sampled Mauritanian isolates does not establish that the virus originated in Mauritania or spread from Mauritania to Guinea. The timing, direction, and number of introduction events remain unresolved.

Previous studies of BUNV have described lytic infection in mammalian cells and persistent infection in mosquito cells [31–35]. In other mosquito cell lines, including C7-10 and U4.4 cells derived from *Aedes albopictus*, BUNV has been reported to persist for 25 passages (approximately 7 months) [31]. In the present study, NRIV infection produced cytopathic effects in the mammalian cell lines, whereas no cytopathic effects were observed in C6/36 cells during the observation period despite the detection of infectious virus. This finding is consistent with the non-cytolytic infection described for related orthobunyaviruses in mosquito cells, although persistent NRIV infection was not established in our experiments. Previous work has also reported limited NRIV replication in other mosquito cell lines [18], indicating that findings in C6/36 cells should not be generalized to all mosquito-derived cells. Likewise, cell-culture findings do not directly establish vector competence, which has been examined separately for selected mosquito species [36]. In TH-1 cells, infectious virus titers were low, and no cytopathic effects were observed. Because samples from the different cell lines were collected at different time points, the measured titers do not provide a direct comparison of replication kinetics. Studies of BUNV have implicated NSs in modulation of host responses [34,35,37–39], providing a possible context for these observations. However, NSs activity was not examined in the present study, and the TH-1 findings do not establish whether NRIV NSs affect host transcription, translation, or interferon responses in reptilian cells. An NSs-related explanation remains an untested hypothesis.

The mouse experiments document disease outcomes following intracerebral and subcutaneous inoculation with the two Guinean NRIV isolates. The outcomes after intracerebral inoculation support neurovirulence under the conditions tested. Following subcutaneous inoculation, infectious virus was recovered from brain samples in Vero cells, with concordant RT-qPCR results. These findings are consistent with the virus reaching the CNS after peripheral inoculation. This interpretation is based on the tissue findings rather than mortality alone. However, the limited sampling does not establish the frequency, kinetics, or route of neuroinvasion, and the study does not demonstrate unusually pronounced neuroinvasive properties.

Published studies illustrate the dependence of orthobunyavirus disease outcomes on the animal model and experimental conditions. In the cited La Crosse virus study, younger mice developed lethal disease, whereas adult mice survived [40]. The Oropouche virus study reported markedly different outcomes in wild-type mice and mice deficient in components of antiviral innate immunity [41]. For a Kenyan NRIV isolate, susceptibility also differed between suckling and adult mice under the conditions examined [42]. These studies provide context for interpreting the outcomes observed with the Guinean isolates, but differences in mouse background, age, immune status, inoculation route, and infectious-dose measurements prevent a direct ranking of the viruses by neurovirulence or neuroinvasiveness. Because no comparator viruses were tested in parallel, the present study does not establish that the Guinean isolates possess greater neurovirulence or neuroinvasiveness than other NRIV strains or related orthobunyaviruses.

This study has several limitations. No a priori sample size calculation was performed, and the small experimental groups limit the precision of estimates and the ability to detect between-strain differences. Between-strain comparisons were exploratory, and non-significant results do not establish equivalence. The isolated nominally significant survival comparison should also be interpreted cautiously in the context of multiple comparisons. Tissue analyses were restricted to two animals per group that died or reached humane endpoints; surviving animals were not examined for tissue distribution. Individual tissue homogenates were examined by RT-qPCR and inoculation of Vero cells before pooling, with concordant results. Infectious virus titration was subsequently performed on pooled samples, and the three replicate assays describe technical variability rather than biological variability between animals. Agreement between the two detection methods supports the reported findings but does not overcome the limited biological sample size. No blood sampling for viremia assessment, systematic tissue time-course, histopathological examination, or analysis of the spinal cord and peripheral nerves was performed. Negative findings in the other examined organs therefore do not exclude infection at levels undetectable under the conditions used or at other stages of disease. Only one inbred mouse strain was used, and male and female outcomes were not analyzed separately. These limitations restrict conclusions about pathogenesis and the generalizability of the findings.

5. Conclusions

In this study, we isolated and characterized two NRIV strains, Tintin and Sabadou, from pools of engorged ixodid ticks collected from cattle in Guinea. Their genome sequences showed close genetic relationships with sampled Mauritanian isolates, without resolving the geographic origin or introduction history of the Guinean strains. Cell-culture and mouse experiments provided descriptive information on the biological properties of the isolates. Detection of infectious virus in brain samples following subcutaneous inoculation was consistent with CNS involvement after peripheral infection, although the limited tissue sampling precluded conclusions about the frequency, kinetics, or route of neuroinvasion. Isolation from engorged ticks does not establish tick vector competence. These findings extend the characterization of NRIV detected in Guinea while leaving its transmission ecology and detailed pathogenesis unresolved.

Supplementary Materials: The following supporting information can be downloaded at: https://www.mdpi.com/article/10.3390/microorganisms14122751/s1, Table S1: Primers used for amplification and sequencing of the NRIV genomes; Table S2: Individual survival data for adult BALB/c mice, including PBS controls; Table S3: Individual survival data for suckling BALB/c mice, including PBS controls.

Author Contributions: Conceptualization, R.B.B., E.V.P., V.A.S.; methodology, R.B.B., E.V.P., A.V.G., V.A.S., M.T.M., L.S.K.; investigation and data collection, R.B.B., E.V.P., A.V.G., V.A.S., M.T.M., L.S.K., V.A.T.; statistical analysis, M.T.M., R.B.B., V.A.S.; writing—original draft preparation, R.B.B., V.A.S.; writing—review and editing, R.B.B., M.T.M., V.A.S., E.V.P., V.A.T., L.S.K.; supervision, S.B., V.A.T., A.P.A.; project administration, V.A.T., A.P.A., and S.B. All authors have read and agreed to the published version of the manuscript.

Funding: The research was funded by the budget of the FBSI SRC of Virology and Biotechnology Vector. The funder had no role in the design, analysis or reporting of the study.

Institutional Review Board Statement: All procedures with the animals were carried out in accordance with the current documents "Rules for carrying out work using experimental animals" (https://docs.cntd.ru/document/456016716, accessed on 21 April 2021) and "Guide for the care and use of laboratory animals" [20], and also in accordance with protocol No. 1-04.2021, approved by the Bioethics Commission of the SRC VB «Vector» on 30 April 2021.

Informed Consent Statement: Not applicable.

Data Availability Statement: The genome sequences are available in GenBank under accession numbers MT929317–MT929322. Individual animal survival data, including observation times and event indicators for experimental and PBS control groups, are provided in Supplementary Tables S2 and S3. Other data supporting the reported findings are included in the article and its Supplementary Materials.

Conflicts of Interest: The authors declare no conflicts of interest.

References

1. Abudurexiti, A.; Adkins, S.; Alioto, D.; Alkhovsky, S.V.; Avšič-Županc, T.; Ballinger, M.J.; Bente, D.A.; Beer, M.; Bergeron, É.; Blair, C.D.; et al. Taxonomy of the Order *Bunyavirales*: Update 2019. *Arch. Viral.* **2019**, *164*, 1949–1965. [CrossRef] [PubMed]
2. Yanase, T.; Kato, T.; Yamakawa, M.; Takayoshi, K.; Nakamura, K.; Kokuba, T.; Tsuda, T. Genetic Characterization of Batai Virus Indicates a Genomic Reassortment between *Orthobunyaviruses* in Nature. *Arch. Virol.* **2006**, *151*, 2253–2260. [CrossRef] [PubMed]
3. Kokernot, R.H.; Smithburn, K.C.; de Meillon, B.; Paterson, H.E. Isolation of Bunyamwera Virus from a Naturally Infected Human Being and Further Isolations from *Aedes (Banksinella) Circumluteolus* Theo. *Am. J. Trop. Med. Hyg.* **1958**, *7*, 579–584. [CrossRef] [PubMed]
4. Tauro, L.B.; Rivarola, M.E.; Lucca, E.; Mariño, B.; Mazzini, R.; Cardoso, J.F.; Barrandeguy, M.E.; Teixeira Nunes, M.R.; Contigiani, M.S. First Isolation of Bunyamwera Virus (*Bunyaviridae* Family) from Horses with Neurological Disease and an Abortion in Argentina. *Vet. J.* **2015**, *206*, 111–114. [CrossRef] [PubMed]
5. Jäckel, S.; Eiden, M.; El Mamy, B.O.; Isselmou, K.; Vina-Rodriguez, A.; Doumbia, B.; Groschup, M.H. Molecular and Serological Studies on the Rift Valley Fever Outbreak in Mauritania in 2010. *Transbound. Emerg. Dis.* **2013**, *60*, 31–39. [CrossRef] [PubMed]
6. Bowen, M.D.; Trappier, S.G.; Sanchez, A.J.; Meyer, R.F.; Goldsmith, C.S.; Zaki, S.R.; Dunster, L.M.; Peters, C.J.; Ksiazek, T.G.; Nichol, S.T. A Reassortant Bunyavirus Isolated from Acute Hemorrhagic Fever Cases in Kenya and Somalia. *Virology* **2001**, *291*, 185–190. [CrossRef] [PubMed]
7. Mhamadi, M.; Dieng, I.; Dolgova, A.S.; Touré, C.T.; Ndiaye, M.; Diagne, M.M.; Faye, B.; Gladkikh, A.S.; Dedkov, V.G.; Sall, A.A.; et al. Whole Genome Sequencing Analysis of African *Orthobunyavirus* Isolates Reveals Naturally Interspecies Segments Recombinations between Bunyamwera and Ngari Viruses. *Viruses* **2023**, *15*, 550. [CrossRef] [PubMed]
8. Eiden, M.; Vina-Rodriguez, A.; El Mamy, B.O.; Isselmou, K.; Ziegler, U.; Höper, D.; Jäckel, S.; Balkema-Buschmann, A.; Unger, H.; Doumbia, B.; et al. Ngari Virus in Goats during Rift Valley Fever Outbreak, Mauritania, 2010. *Emerg. Infect. Dis.* **2014**, *20*, 2174–2176. [CrossRef] [PubMed]
9. Cichon, N.; Barry, Y.; Stoek, F.; Diambar, A.; Ba, A.; Ziegler, U.; Rissmann, M.; Schulz, J.; Haki, M.L.; Höper, D.; et al. Co-Circulation of *Orthobunyaviruses* and Rift Valley Fever Virus in Mauritania, 2015. *Front. Microbiol.* **2021**, *12*, 766977. [CrossRef] [PubMed]
10. Briese, T.; Bird, B.; Kapoor, V.; Nichol, S.T.; Lipkin, W.I. Batai and Ngari Viruses: M Segment Reassortment and Association with Severe Febrile Disease Outbreaks in East Africa. *J. Virol.* **2006**, *80*, 5627–5630. [CrossRef] [PubMed]
11. Gerrard, S.R.; Li, L.; Barrett, A.D.; Nichol, S.T. Ngari Virus Is a Bunyamwera Virus Reassortant That Can Be Associated with Large Outbreaks of Hemorrhagic Fever in Africa. *J. Virol.* **2004**, *78*, 8922–8926. [CrossRef] [PubMed]
12. Gordon, S.W.; Tammariello, R.F.; Linthicum, K.J.; Dohm, D.J.; Digoutte, J.P.; Calvo-Wilson, M.A. Arbovirus Isolations from Mosquitoes Collected during 1988 in the Senegal River Basin. *Am. J. Trop. Med. Hyg.* **1992**, *47*, 742–748. [CrossRef] [PubMed]
13. Zeller, H.G.; Diallo, M.; Angel, G.; Traore-Lamizana, M.; Thonnon, J.; Digoutte, J.P.; Fontenille, D. Ngari Virus (*Bunyaviridae*: Bunyavirus). First Isolation from Humans in Senegal, New Mosquito Vectors, Its Epidemiology. *Bull. Soc. Pathol. Exot.* **1996**, *89*, 12–16. [PubMed]
14. Ochieng, C.; Lutomiah, J.; Makio, A.; Koka, H.; Chepkorir, E.; Yalwala, S.; Mutisya, J.; Musila, L.; Khamadi, S.; Richardson, J.; et al. Mosquito-Borne Arbovirus Surveillance at Selected Sites in Diverse Ecological Zones of Kenya; 2007–2012. *Virol. J.* **2013**, *10*, 140. [CrossRef] [PubMed]
15. Makenov, M.T.; Toure, A.H.; Bayandin, R.B.; Gladysheva, A.V.; Shipovalov, A.V.; Boumbaly, S.; Sacko, N.; Korneev, M.G.; Yakovlev, S.A.; Zhurenkova, O.B.; et al. Ngari Virus (*Orthobunyavirus*, Peribunyaviridae) in Ixodid Ticks Collected from Cattle in Guinea. *Acta Trop.* **2021**, *214*, 105790. [CrossRef] [PubMed]
16. Odhiambo, C.; Venter, M.; Lwande, O.; Swanepoel, R.; Sang, R. Phylogenetic Analysis of Bunyamwera and Ngari Viruses (Family *Bunyaviridae*, Genus *Orthobunyavirus*) Isolated in Kenya. *Epidemiol. Infect.* **2016**, *144*, 389–395. [CrossRef] [PubMed]
17. Dutuze, M.F.; Nzayirambaho, M.; Mores, C.N.; Christofferson, R.C. A Review of Bunyamwera, Batai, and Ngari Viruses: Understudied *Orthobunyaviruses* with Potential One Health Implications. *Front. Vet. Sci.* **2018**, *5*, 69. [CrossRef] [PubMed]
18. Omoga, D.C.A.; Tchouassi, D.P.; Venter, M.; Ogola, E.O.; Eibner, G.J.; Kopp, A.; Slothouwer, I.; Torto, B.; Junglen, S.; Sang, R. Circulation of Ngari Virus in Livestock, Kenya. *mSphere* **2022**, *7*, e00416-22. [CrossRef] [PubMed]

19. Lei, C.; Yang, J.; Hu, J.; Sun, X. On the Calculation of $TCID_{50}$ for Quantitation of Virus Infectivity. *Virol. Sin.* **2021**, *36*, 141–144. [CrossRef] [PubMed]
20. National Research Council. *Guide for the Care and Use of Laboratory Animals*, 8th ed.; National Academies Press: Washington, DC, USA, 2011. [CrossRef] [PubMed]
21. Percie du Sert, N.; Ahluwalia, A.; Alam, S.; Avey, M.T.; Baker, M.; Browne, W.J.; Clark, A.; Cuthill, I.C.; Dirnagl, U.; Emerson, M.; et al. Reporting Animal Research: Explanation and Elaboration for the ARRIVE Guidelines 2.0. *PLoS Biol.* **2020**, *18*, e3000411. [CrossRef] [PubMed]
22. Dolgova, A.S.; Safonova, M.V.; Faye, O.; Dedkov, V.G. Current View on Genetic Relationships within the Bunyamwera Serological Group. *Viruses* **2022**, *14*, 1135. [CrossRef] [PubMed]
23. Kumar, S.; Stecher, G.; Li, M.; Knyaz, C.; Tamura, K. MEGA X: Molecular Evolutionary Genetics Analysis across Computing Platforms. *Mol. Biol. Evol.* **2018**, *35*, 1547–1549. [CrossRef] [PubMed]
24. Hoang, D.T.; Chernomor, O.; Von Haeseler, A.; Minh, B.Q.; Vinh, L.S. UFBoot2: Improving the Ultrafast Bootstrap Approximation. *Mol. Biol. Evol.* **2018**, *35*, 518–522. [CrossRef] [PubMed]
25. Nguyen, L.T.; Schmidt, H.A.; Von Haeseler, A.; Minh, B.Q. IQ-TREE: A Fast and Effective Stochastic Algorithm for Estimating Maximum-Likelihood Phylogenies. *Mol. Biol. Evol.* **2015**, *32*, 268–274. [CrossRef] [PubMed]
26. Therneau, T.M. A Package for Survival Analysis in R. 2026. Available online: https://CRAN.R-project.org/package=survival (accessed on 30 October 2026).
27. Kassambara, A.; Kosinski, M.; Biecek, P. *survminer*: Drawing Survival Curves Using ggplot2. 2026. Available online: https://CRAN.R-project.org/package=survminer (accessed on 30 October 2026).
28. Wickham, H. *ggplot2: Elegant Graphics for Data Analysis*; Springer: New York, NY, USA, 2009. [CrossRef]
29. Lwande, O.W.; Lutomiah, J.; Obanda, V.; Gakuya, F.; Mutisya, J.; Mulwa, F.; Michuki, G.; Chepkorir, E.; Fischer, A.; Venter, M.; et al. Isolation of Tick and Mosquito-Borne Arboviruses from Ticks Sampled from Livestock and Wild Animal Hosts in Ijara District, Kenya. *Vector Borne Zoonotic Dis.* **2013**, *13*, 637–642. [CrossRef] [PubMed]
30. Kolodziejek, J.; Marinov, M.; Kiss, B.J.; Alexe, V.; Nowotny, N. The Complete Sequence of a West Nile Virus Lineage 2 Strain Detected in a *Hyalomma marginatum marginatum* Tick Collected from a Song Thrush (*Turdus philomelos*) in Eastern Romania in 2013 Revealed Closest Genetic Relationship to Strain Volgograd 2007. *PLoS ONE* **2014**, *9*, e109905. [CrossRef] [PubMed]
31. Szemiel, A.M.; Failloux, A.B.; Elliott, R.M. Role of Bunyamwera *Orthobunyavirus* NSs Protein in Infection of Mosquito Cells. *PLoS Negl. Trop. Dis.* **2012**, *6*, e1823. [CrossRef] [PubMed]
32. Newton, S.E.; Short, N.J.; Dalgarno, L. Bunyamwera Virus Replication in Cultured *Aedes albopictus* (Mosquito) Cells: Establishment of a Persistent Viral Infection. *J. Virol.* **1981**, *38*, 1015–1024. [CrossRef] [PubMed]
33. Scallan, M.F.; Elliott, R.M. Defective RNAs in Mosquito Cells Persistently Infected with Bunyamwera Virus. *J. Gen. Virol.* **1992**, *73*, 53–60. [CrossRef] [PubMed]
34. Kohl, A.; Clayton, R.F.; Weber, F.; Bridgen, A.; Randall, R.E.; Elliott, R.M. Bunyamwera Virus Nonstructural Protein NSs Counteracts Interferon Regulatory Factor 3-Mediated Induction of Early Cell Death. *J. Virol.* **2003**, *77*, 7999–8008. [CrossRef] [PubMed]
35. Hart, T.J.; Kohl, A.; Elliott, R.M. Role of the NSs Protein in the Zoonotic Capacity of *Orthobunyaviruses*. *Zoonoses Public Health* **2009**, *56*, 285–296. [CrossRef] [PubMed]
36. Odhiambo, C.; Venter, M.; Chepkorir, E.; Mbaika, S.; Lutomiah, J.; Swanepoel, R.; Sang, R. Vector Competence of Selected Mosquito Species in Kenya for Ngari and Bunyamwera Viruses. *J. Med. Entomol.* **2014**, *51*, 1248–1253. [CrossRef] [PubMed]
37. Bridgen, A.; Weber, F.; Fazakerley, J.K.; Elliott, R.M. Bunyamwera Bunyavirus Nonstructural Protein NSs Is a Nonessential Gene Product That Contributes to Viral Pathogenesis. *Proc. Natl. Acad. Sci. USA* **2001**, *98*, 664–669. [CrossRef] [PubMed]
38. Van Knippenberg, I.; Carlton-Smith, C.; Elliott, R.M. The N-Terminus of Bunyamwera *Orthobunyavirus* NSs Protein Is Essential for Interferon Antagonism. *J. Gen. Virol.* **2010**, *91*, 2002–2006. [CrossRef] [PubMed]
39. Weber, F.; Bridgen, A.; Fazakerley, J.K.; Streitenfeld, H.; Kessler, N.; Randall, R.E.; Elliott, R.M. Bunyamwera Bunyavirus Nonstructural Protein NSs Counteracts the Induction of Alpha/Beta Interferon. *J. Virol.* **2002**, *76*, 7949–7955. [CrossRef] [PubMed]
40. Alatrash, R.; Vaidya, V.; Herrera, B.B. Age-Specific Dynamics of Neutralizing Antibodies, Cytokines, and Chemokines in Response to La Crosse Virus Infection in Mice. *J. Virol.* **2024**, *98*, e01762-24. [CrossRef] [PubMed]
41. Proenca-Modena, J.L.; Sesti-Costa, R.; Pinto, A.K.; Richner, J.M.; Lazear, H.M.; Lucas, T.; Hyde, J.L.; Diamond, M.S. Oropouche Virus Infection and Pathogenesis Are Restricted by MAVS, IRF-3, IRF-7, and Type I Interferon Signaling Pathways in Nonmyeloid Cells. *J. Virol.* **2015**, *89*, 4720–4737. [CrossRef] [PubMed]
42. Odhiambo, C.; Venter, M.; Limbaso, K.; Swanepoel, R.; Sang, R. Genome Sequence Analysis of in Vitro and in Vivo Phenotypes of Bunyamwera and Ngari Virus Isolates from Northern Kenya. *PLoS ONE* **2014**, *9*, e105446. [CrossRef] [PubMed]

Disclaimer/Publisher's Note: The statements, opinions and data contained in all publications are solely those of the individual author(s) and contributor(s) and not of MDPI and/or the editor(s). MDPI and/or the editor(s) disclaim responsibility for any injury to people or property resulting from any ideas, methods, instructions or products referred to in the content.